PCCP

ROYAL SOCIETY OF CHEMISTRY

PAPER

View Article Online
View Journal | View Issue

Cite this: *Phys. Chem. Chem. Phys.*, 2022, **24**, 5590

Orbital-dependent photodynamics of strongly correlated nickel oxide clusters†

Jacob M. Garcia [ab] and Scott G. Sayres *[ab]

Received 14th January 2022,
Accepted 11th February 2022

DOI: 10.1039/d2cp00209d

rsc.li/pccp

The ultrafast electronic relaxation dynamics of neutral nickel oxide clusters were investigated with femtosecond pump–probe spectroscopy and supported with theoretical calculations to reveal that their excited state lifetimes are strongly dependent on the nature of the electronic transition. Absorption of a UV photon produces short-lived (lifetime ~ 110 fs) dynamics in stoichiometric $(NiO)_n$ clusters ($n < 6$) that are attributed to a ligand to metal charge transfer (LMCT) and produces metallic-like electron–electron scattering. Oxygen vacancies introduce excitations with Ni-3d → Ni-4s and 3d → 4p character, which increases the lifetimes of the sub-picosecond response by up to 80% and enables the formation of long-lived (lifetimes >2.5 ps) states. The atomic precision and tunability of gas phase clusters are employed to highlight a unique reliance on the Ni orbital contributions to the photoexcited lifetimes, providing new insights to the analogous band edge excitation dynamics of strongly correlated bulk-scale NiO materials.

1. Introduction

In strongly correlated materials, such as transition metal oxides, the electronic structure reflects the coupling between the orbital, spin, and charge degrees of freedom. This leads to numerous competing metastable phases that are accessible *via* ultrafast photoexcitation and are important in opto-electronics and light harvesting. The local rearrangement of the 3d-electrons plays a crucial role in many properties of correlated transition metal oxide materials and supplies information on magnetic interactions. NiO is the prototypical strongly correlated material, whose electronic structure has been a topic of interest for decades owing to its potential to serve in numerous energy applications as an efficiency-enhancing interfacial layer[1] and as a hole transport layer in photovoltaic[2] and dye sensitized solar cells.[3] NiO is also antiferromagnetic with a high Néel temperature of 523 K,[4–6] making it a strong candidate for spintronic devices. Photoexcitation of NiO can invoke a ferromagnetic response,[5–8] and alter its insulator-like properties on ultrafast timescales.[9] Ultimately, the timescale that NiO redistributes photoexcitation and the related mechanism of local rearrangement of 3d-electrons dictate its activity in solar cell applications and its efficiency as opto-electronic and opto-magnetic devices.

Ni has the lowest excitation energy of the first-row transition metal elements and an open 3d subshell, providing an extremely rich density of states. This enables electron–electron (e–e) scattering to be a prominent relaxation mechanism in bulk NiO, leading to excited state dynamics as short as 10s of fs[7,10] and polaron formation on the sub-ps timescale.[11] The d^8 ground state electron configuration of NiO formally consists of fully occupied t_{2g} and half-filled e_g orbitals, with strong hybridization between the 2p and 3d bands.[7] The d-shell of Ni is the most compact of all transition metals,[12] enabling NiO to contain signatures of both localized atomic-like states and band-like dispersive electronic states. NiO is classified as an intermediate charge-transfer insulator, suggesting that the charge transfer energy gap (Δ) between the O-2p band and the unoccupied Hubbard band, is smaller than the weakly screened Coulomb interaction (Hubbard U),[7] thereby leaving O-2p bands in the energy range of the occupied Hubbard band. Although the commonly reported band gap of NiO is 4.1–4.3 eV,[8,9] the onset of its photoabsorption has been recorded as low as 3.1 eV.[13] This lower energy feature is often ignored, but has been identified as excitation between the valence Ni-3d and the Ni-4s character of the conduction band minima.[13] Detailed calculations provide mounting support for the importance of such s character states, which are more delocalized.[14,15] This challenges conventional knowledge which considers only localized 3d (e_g) states in the conduction band

[a] *School of Molecular Sciences, Arizona State University, Tempe, AZ 85287, USA. E-mail: Scott.Sayres@asu.edu*
[b] *Biodesign Center for Applied Structural Discovery, Arizona State University, Tempe, AZ 85287, USA*

† Electronic supplementary information (ESI) available: Fig. 1 shows the experimental apparatus, Fig. S2–S4 shows the calculated excited state orbital contributions for nickel oxide clusters. Fig. S5 shows the shows the lifetime measurements for several larger clusters. The *XYZ* coordinates of all clusters are also presented. Fig. S6 presents the cluster structures and spin states. See DOI: 10.1039/d2cp00209d

edge and suggests that the photodynamics of NiO materials are influenced by the involvement of different electronic orbitals.

Sub-nanometer sized clusters are the ideal venue for identifying the electronic and structural factors that govern carrier dynamics and related excited state lifetimes.[16–18] Their electronic properties change with the addition or subtraction of a single atom and their finite size is completely addressable by density functional theory (DFT), enabling detailed insights about the role of defect sites in bulk-scale reactions. Nickel oxide clusters are among the least understood transition metal oxides and are also the most intriguing because they contain a high number of energetically competitive structural isomers and spin configurations. Here, femtosecond pump–probe spectroscopy coupled with theoretical calculations are used to show a unique reliance on the Ni orbital contributions to the photoexcited neutral nickel oxide cluster lifetimes, and by extension allow for a deeper understanding of the bulk-scale photoexcitation. Specifically, we show that the electron transfer from a O-2p orbital to a Ni-3d orbital, commonly referred to as ligand-to-metal charge transfer (LMCT) excitation,[7,15] undergoes rapid relaxation through e–e scattering. The introduction of O vacancies enables Ni-3d → Ni-4s transitions and Ni-3d → Ni-4p transitions that exhibit delocalized carriers and slower relaxation dynamics. We demonstrate these intriguing effects by adjusting the electronic structure of clusters with atomic precision.

2. Experimental methods

Neutral nickel oxide clusters are produced using a laser vaporization source and their excited states are subsequently measured through the pump–probe technique, where ionization enables detection using a home-built Wiley–McLaren[19] type time-of-flight mass spectrometer (TOFMS) discussed in detail previously (Fig. S1, ESI†).[16] Briefly, a pulsed Nd:YAG laser was used for ablation of a pure 1/4″ nickel rod under high vacuum conditions ($\sim 7.5 \times 10^{-8}$ torr). The plasma plume was directed by expansion of a seeded He gas pulse (1% O_2), confined to a 1×60 mm collision region, and skimmed to a collimated molecular beam diameter of 2 mm. All cations and anions were deflected from the beam prior to ionization of the neutral molecular beam by charging the skimmer to +500 V. Neutral clusters were ionized by a sequence of sub-35 fs laser pulses from a Ti:sapphire laser and accelerated by a $\sim$4 kV pulsed electric field. The clusters were focused onto the detector (MCP) using an Einzel lens and separated in time as they traversed a 1.5 m field-free region. The second harmonic of the laser (400 nm, 3.1 eV) was separated from the fundamental 800 nm (1.55 eV) laser, which traversed a programmed delay-stage before recombining the beams. The 800 nm (probe) beam was temporally scanned in 40 fs increments from −600 to 2500 fs relative to the 400 nm (pump) beam. Excitation is achieved with a single pump photon and ionization occurs through absorption of multiple probe photons. All spectra were recorded using 7.92×10^{14} W cm^{-2} 400 nm pump and 1.62×10^{15} W cm^{-2} 800 nm probe pulses. An average of 500 spectra were recorded for each time delay.

The excited state transient signals of neutral nickel oxide clusters are recorded by scanning the optical delay of the probe beam with respect to the pump pulse and tracking the change of intensity from each ion signal. The ion signal is proportional to the excited state population as it decays in time. The 800 nm beam was measured through autocorrelation to be $<$35 fs. The instrumental response function (Gaussian function) is measured to be $<$ 50 fs (FWHM) using the enhancement of non-resonant ionization signal of O_2 that matches the cross correlation. The maximum intensity of the cluster signals is recorded $\sim$50 fs after the temporal overlap of the two laser pulses (time zero). This delay onset of cluster signal reveals that the signal is dominated by direct ionization through a resonant excitation. The transient ion signal is a convolution of the molecular response and the cross-correlation of the two laser beams and therefore the maximum of the ion signal exhibits a temporal shift proportional to the lifetime of the cluster. An exponential decay function and plateau function are used to fit all cluster transients, described in detail previously.[16,17] These are both convoluted with the Gaussian instrumental response function, where the exponential decay function accounts for the fast relaxation in transient signals associated with an intermediate metastable state of a neutral cluster that decays with the measured lifetime (τ) and the plateau function represents a stable long-lived ($>$2.5 ps) excited state that survives longer than the experiment.

3. Computational methods

DFT calculations are performed to relate the experimental lifetimes to the electronic properties of each cluster. Due to the accuracy demonstrated by BPW91 previously for both nickel and nickel oxide clusters, and for both low computational cost and high speed, we rely on the GGA functional uBPW91[20] to calculate the nickel oxide clusters. Often BPW91 performs better than B3LYP for describing magnetic properties because the XC functional LYP does not have equal spin correlation and exaggerates the opposite-spin correlation,[21] which plays a strong role in the high spin structures of the nickel oxide clusters. Calculations were performed using the 6-311G+* basis set, namely (15s11p6d1f/10s7p4d1f) for Ni and (12s6p1d/5s4p1d) for O atoms. The initial choices for the atomic coordinates for the geometry optimizations were obtained from previous studies[22,23] and then optimized in Gaussian16[24] while considering a variety of spin states (up to $2S + 1 = 13$). Our calculated structures of nickel oxide clusters are in agreement with previous calculations, and show that $(NiO)_{2-5}$ clusters all form planar ring structures. Suboxides show strong Ni–Ni bonding, with O atoms decorating the periphery of the cluster in hollow sites followed by bridging locations, avoiding O–O bonding and terminal O sites. The optimized neutral cluster structures are presented next to their transient signals.

Although the cluster distribution may contain several isomers, especially for larger clusters, the lowest energy configuration is likely dominant and can provide insight to the excited state dynamics. Thus, the lowest energy spin configuration and geometries were used as input for single point time dependent-density functional theory (TD-DFT) calculations to account for the excited state characteristics. A sufficient number of excited states are included for each cluster to exceed the pump photon energy (400 nm = 3.1 eV). An excited state population analysis was performed to determine the elemental contributions to the excited state nearest 3.1 eV. The C-squared population analysis (CSPA) method disregards the fact that basis functions may overlap, and simply defines the contribution, c_{ai}, of a particular atomic orbital, a, to a particular molecular orbital, i, as the square of the molecular orbital coefficient normalized to the square of all atomic orbital coefficients, k, as:

$$\phi_{ai} = \frac{{c_{ai}}^2}{\sum_k {c_{ki}}^2}. \quad (1)$$

Several occupied virtual pairs contribute to a given TD-DFT excitation, and the contribution coefficient of each pair, C_{ai}, is output by Gaussian16. It should be noted that the maximum total electron density transferred from a photoexcitation is 1, but the linear combination of several occupied-virtual pairs that contribute to the photoexcitation can reduce this value. Thus, values less than 1 indicate conflict between orbital pairs (the individual excitations cancel one another for no net change between atomic orbitals), or excitation within the d–d orbitals occurs. Photoexcitation is characterized as the change in electron density on each of the Ni-3d, Ni-4s, Ni-4p, and O-2p orbitals. The Ni-f, O-s, and O-d orbitals are also calculated, but are not reported because they do not compose a significant percentage of the charge transfer.

4. Results and discussion

The measured cluster distribution is presented in Fig. 1. The prominent neutral clusters are the Ni_nO_{n-1} series from values of $n < 8$ and then Ni_nO_{n-2} for $n > 7$, consistent with previous experiments.[25,26] Stoichiometric clusters are only recorded for $n \leq 5$. Minor signals from pure nickel clusters, Ni_2 and Ni_3, also appear in the neutral mass spectrum.

The transients of the $(NiO)_n$ clusters (n = 1–5) all show a similar fast relaxation of ~110 fs following absorption of a single UV (400 nm = 3.1 eV) photon (Fig. 2). Our calculations (Table 1) reveal that in all cases, photoexcitation involves a transition from the O atoms to the Ni atoms in a LMCT. The electron density on the Ni atoms increases through photoexcitation and therefore exhibits a fast relaxation that is attributed to e–e scattering, similar to bulk NiO. The slightly longer lifetime of NiO over larger stoichiometric clusters is due to a lower density of states and degrees of freedom. The fraction of the excited state population (δ) that enters a long-lived (>2.5 ps) state, determined by the amplitude ratio of the fitting coefficients between the plateau function and total transient signal, reveals a decrease in the long-lived component with size of stoichiometric cluster (Table 1). A long-lived state is accessible in NiO (δ = 18%) and $(NiO)_2$ (δ = 2.0%) but is not in larger clusters. The decreasing plateau component of the transient signal suggests that the larger clusters contain sufficiently high

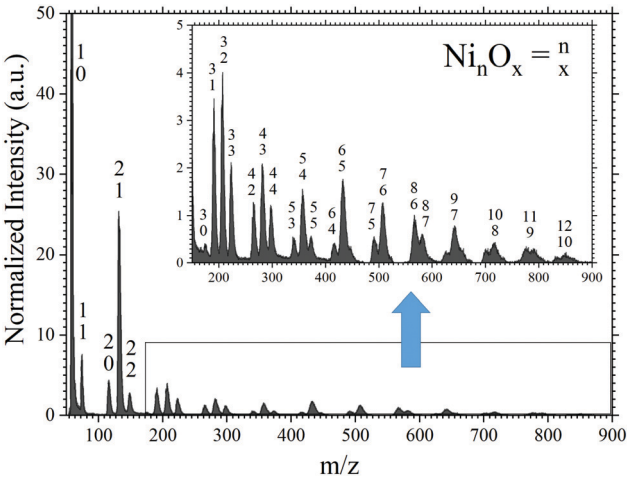

Fig. 1 Mass spectrum of neutral nickel oxide clusters following photoionization of the pump–probe pulse at temporal overlap. The inset is a zoomed in to show the distribution of the larger clusters.

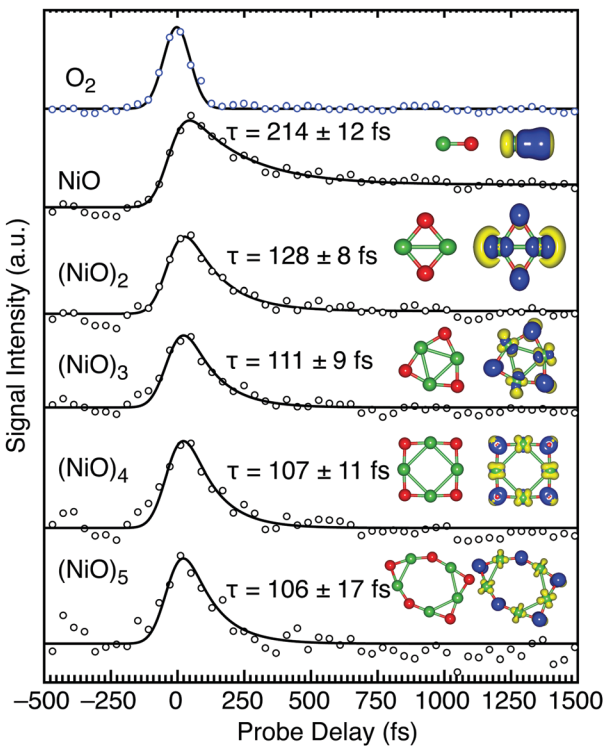

Fig. 2 Transient signals of $(NiO)_n$ (n = 1–5) clusters with total fit shown in black and lifetime shown above each curve. The non-resonant ionization signal of O_2 is shown as blue circles. TD-DFT BPW91 transition densities are presented at an isodensity of 0.005 $Å^{-3}$. Electron densities are yellow, holes are blue, Ni atoms are green, and O atoms are red.

Table 1 Excited state lifetimes (τ), long-lived percent population (δ), and changes in electron density for each atomic orbital for neutral $(NiO)_n$ clusters (n = 1–5)

Cluster	τ (fs)	δ (%)	Ni-3d	Ni-4p	Ni-4s	O-2p
NiO	214 ± 12	18	4	3.1	0	−7
$(NiO)_2$	128 ± 8	2.0	−62	15	66	−29
$(NiO)_3$	111 ± 9	0.0	15	−6	28	−38
$(NiO)_4$	107 ± 11	0.0	24	−6	−3	−21
$(NiO)_5$	106 ± 17	0.0	39	−5	42	−77

density of states to enable charge recombination. The potential energy curves of NiO reveal a rich density of excited states below the $X^3\Sigma^- \rightarrow {}^3\Sigma^-$ photoexcitation at 3.04 eV.[27] Photoelectron spectroscopy (PES) of NiO shows several low-lying excited states below 3 eV,[28–31] and a ~0.5 eV energy gap between the ground and the first excited state.[27,32] Our measurements show the $^3\Sigma^-$ state of NiO has a lifetime of 214 ± 12 fs and may cross into a long-lived $^3\Sigma^+$ or $^3\Delta$ state, which is represented by the plateau function. This is in agreement with literature results, where lower lying excited states exhibit microsecond lifetimes following visible excitation.[33] Perhaps unsurprisingly, the stoichiometric clusters exhibit the fastest lifetimes due to the LMCT placing more electron density on the Ni-3d orbitals which relax through e–e scattering. These results echo the rapid relaxation dynamics reported for chromium oxide clusters, where the LMCT character of the excited state is proportional to the 10s of fs relaxation through e–e scattering amongst the d electrons.[18] The e–e scattering mechanism is likely prominent in all open d-shell transition metal oxides, especially when LMCT occurs.

Oxygen deficient clusters possess longer sub-ps lifetimes (by up to 80%) than the stoichiometric series (Table 2). Such suboxides have large proportions of 3d → 4p photoexcitation which may be responsible for the long-lived states. The Ni_2O_x ($x < 3$) series reveals gradual changes in excited state transients with O content (Fig. 3).

The transient signal for Ni_2 requires a growth function (τ_g) and shows the entire population reaches a long-lived (>2.5 ps)

Table 2 Excited state lifetimes (τ), long-lived percent population (δ), and changes in electron density for each atomic orbital of suboxide neutral nickel oxide clusters

Cluster	τ (fs)	δ (%)	Ni-3d	Ni-4p	Ni-4s	O-2p
Ni_2	28 ± 9[a]	100	−97	97	0	—
Ni_2O	204 ± 18	32	−95	32	55	9
Ni_3	170 ± 51[a]	100	−92	92	0	—
Ni_3O	191 ± 18	18	−57	25	28	3
Ni_3O_2	202 ± 23	13	−17	3	−6	20
Ni_4O_2	187 ± 22	4.0	−65	19	39	3
Ni_4O_3	176 ± 20	0.0	−71	24	35	9
Ni_5O_3	117 ± 20	0.0	−71	17	42	4
Ni_5O_4	151 ± 20	0.0	−54	4	43	−15
Ni_6O_4	225 ± 40	0.0	−59	5	39	−14
Ni_6O_5	173 ± 23	0.0	−13	−2	6	10
Ni_7O_5	167 ± 36	0.0	−21	0	15	−8
Ni_7O_6	142 ± 23	0.0	−20	1	7	5

[a] Indicates growth lifetime instead of decay.

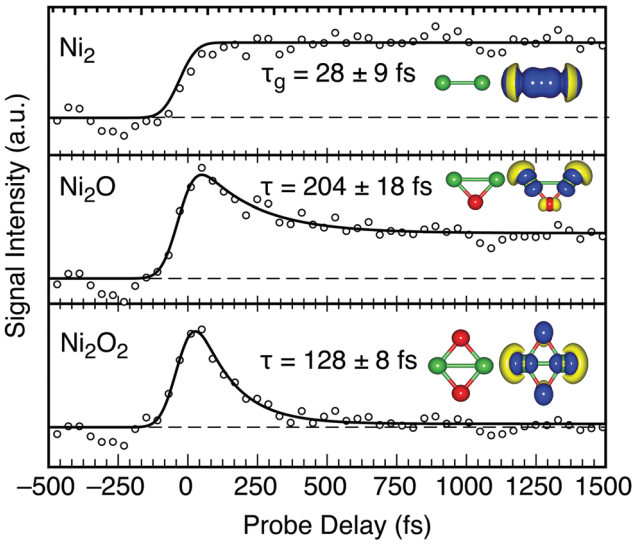

Fig. 3 Transient signals for Ni_2O_x ($x < 3$) clusters with total fit and lifetime shown. Dashed lines show the initial signal intensity. The structures and densities are similar to Fig. 2, except Ni_2 is shown at an isodensity of 0.002 $Å^{-3}$.

state. The measured τ_g (28 ± 9 fs) matches the cross correlation of the laser beams, suggesting the signal arises from the direct ionization of Ni_2 that is present in the neutral cluster population. The ground state of Ni_2 has been investigated with controversial results that arise from the interaction of two $3d^94s^1$ Ni atoms, forming a single bond between the 4s orbitals with little 3d involvement. The electronically excited states are difficult to assign, but appear at wavelengths <450 nm.[34] The UV-vis spectra of Ni_2 shows several absorption bands at ~3 eV.[35,36] The $d\sigma_g \rightarrow p\pi_u$ ($^3\pi_u$ or C state) is strongly bound, but overlaps with the dissociative $s\sigma_g \rightarrow s\sigma_u$ ($^3\Sigma_u^-$ or B state).[35,37] A $d\delta_g \rightarrow p\pi_u$ transition ($^3\Phi_u$ state) may also exist nearby but is expected to have weak signal intensity. No decrease in the transient Ni_2^+ signal is recorded, suggesting the C $^3\pi_u$ state of Ni_2 is accessed by the 3.1 eV pump photon and is long lived due to poor overlap with lower lying states. Photoexcitation of Ni_2 is strictly Ni-3d → Ni-4p in our calculations (Fig. 4). Thus, an electron is promoted from an essentially nonbonding 3d-type molecular orbital into a 4p π_u orbital, with some bonding character resulting in a stronger bond.[38]

The density of states of Ni_2O_2 and Ni_2O (Fig. 4) are in agreement with previous calculations.[39,40] Ni_2O^+ is a particularly stable cation.[25,41] The transient signal for Ni_2O contains a slower (204 ± 18 fs) relaxation, extended by ~60% over Ni_2O_2 which contains a fast (~128 fs) decay from high LMCT. A large proportion (δ = 32%) of the photoexcited Ni_2O population reaches a long-lived state which survives over 2.5 ps, proportional to the amount of d → p transition character. Strong hybridization of Ni-3d and O-2p orbitals enables photoexcitation of Ni_2O to be characterized as Ni-3d → 55% Ni-4s and 32% Ni-4p. The 4s orbitals have favorable exchange interactions with the Ni-3d electrons due to large spatial overlap and are therefore strongly coupled and enable rapid relaxation through

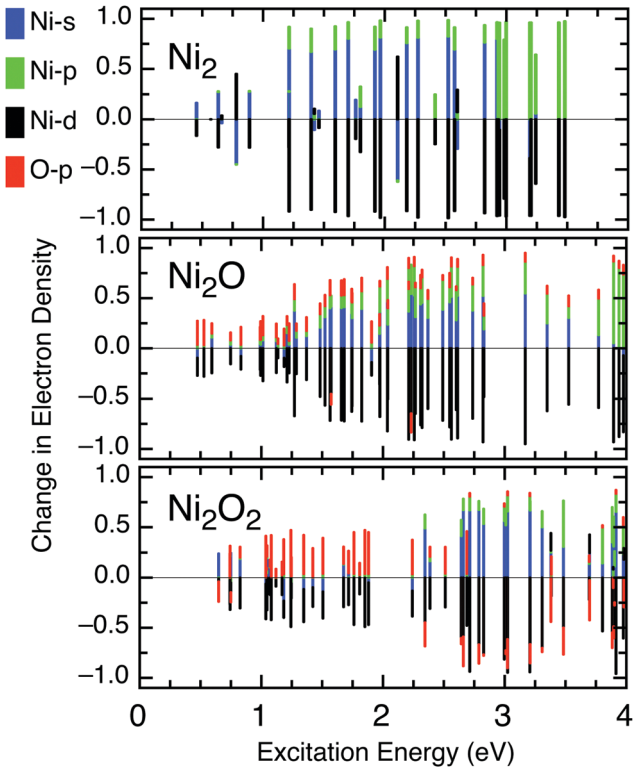

Fig. 4 C-Squared population analysis of the TD-DFT excited states showing the density of states and change in electron density for the Ni-s, Ni-p, Ni-d, and Ni-p orbitals for each of the Ni_2O_x ($x < 3$) clusters.

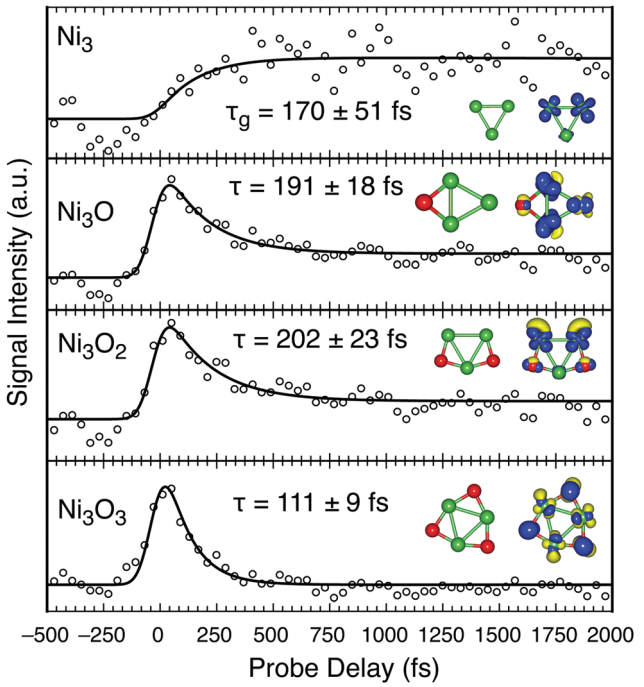

Fig. 5 Transient signal of Ni_3O_x ($x < 4$) clusters and their structures, similar to Fig. 2.

scattering, although slightly slower than the LMCT dynamics of the stoichiometric clusters.

The Ni_3O_x ($x < 4$) clusters behave similar to the Ni_2O_x clusters in that the sub-ps transient lifetime and long-lived (>2.5 ps) excited state population increases with decreased O character (Fig. 5). Ni_3O_x clusters also contain a large density of states, with no obvious energy gaps (Fig. S2, ESI†). The stoichiometric cluster, Ni_3O_3, has the shortest lifetime of the series (111 ± 9 fs) and does not contain a long-lived plateau. With one less O atom, the lifetime of Ni_3O_2 (202 ± 23 fs) increases by ~80% over the stoichiometric cluster. The transient signals for the photoexcitation of Ni_3O_2 and Ni_3O exhibit comparable lifetimes and δ coefficients, suggesting similar excited state landscapes. Our calculations reveal that photoexcitation of both clusters contain significant Ni-3d to Ni-4s and Ni-4p transitions. The 4s component couples to the 3d electrons for a rapid relaxation. Further, the 4s character is larger than the 4p component, reflected by long-lived states that is only 13 and 18% of the total population of the Ni_3O_2 and Ni_3O clusters, respectively.

The excited states of Ni_3 are similar to Ni_2,[35,37] with $d\pi_g \rightarrow p\pi_u$ (bound) and the slightly higher energy $s\sigma_u \rightarrow s\sigma_g$ (dissociative) transitions near 400 nm. However, in contrast to Ni_2^+, the Ni_3^+ signal in our experiment does not appear with the laser pulse but instead exhibits a delayed growth. This delayed transient response is a strong signature of ionization that competes with photodissociation. Several possibilities might account for the growth recorded in the Ni_3^+ signal ($\tau_g = 170 \pm 51$ fs) as it matches closely with the decay lifetime for most clusters, including Ni_3O (~191 ± 18 fs). Our calculations predict a bond dissociation energy of 4.2 eV for Ni_3O, in agreement with literature values,[42] suggesting that it is stable and does not release O to form Ni_3. Photodissociation of Ni_3O_2 to form Ni_3 is unlikely, requiring removal of two O atoms. However, Ni_3^+ is not observed from the photofragmentation of oxygen rich nickel oxide cation clusters[25] and Ni_3^+ has a small fragmentation energy.[43] Thus, it is likely that Ni_3 dissociates into Ni_2 + Ni from the combined energy of both laser beams at temporal overlap, through the dissociative $s\sigma_u \rightarrow s\sigma_g$ excitation channel. This intermediate neutral state crosses into the stable $d\pi_g \rightarrow p\pi_u$ channel in ~170 fs where it remains for the duration of the experiment (2.5 ps). Ionization then proceeds through the removal of the excited nonbonding d electron, resulting in a stable cation.

Clusters containing either 4 or 5 Ni atoms continue to follow the described trend, where the stoichiometric clusters exhibit the fastest relaxation ($\tau \sim 107$ fs) through LMCT, and inclusion of O vacancies enable longer lifetimes. With one less O atom from Ni_4O_4, the lifetime increases by 65% (Fig. 6). The photoexcitation of Ni_4O_3 and Ni_4O_2 contain similar Ni-d → Ni-s and Ni-d → Ni-p character, facilitating similar extended excited state lifetimes ($\tau \sim 180$ fs). Similarly, Ni_5O_3 and Ni_5O_4 contain similar dynamics, with lifetimes slightly longer than Ni_5O_5. The charge transfer of these clusters shows similar effects, where the Ni_5O_3 and Ni_5O_4 clusters are strongly Ni-d → Ni-s. Thus, in the 3D geometry of such larger clusters, the Ni-4p character of the excited electron becomes negligible, and no long-lived signal is obtained, demonstrating an efficient relaxation (Fig. S3, ESI†).

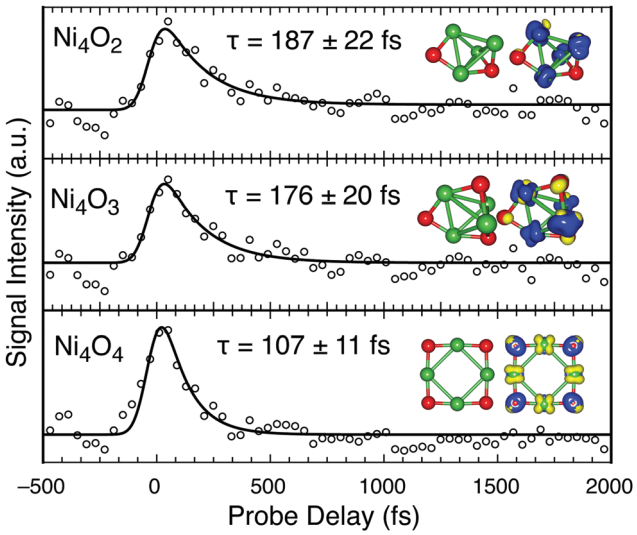

Fig. 6 Transient signal of Ni_4O_x ($x < 4$) clusters and their structures, similar to Fig. 2.

Stoichiometric clusters are not recorded with significant intensity above $(NiO)_5$, however, the similar lifetime values and dynamics measured for a few additional suboxide clusters implies that the trend extends into larger clusters as well. The d → p transition is also not prominent in larger clusters, which instead show mainly a transition of Ni-3d → Ni-4s character. The excited state orbital characters and change in electron transition densities for Ni_6O_{4-5} and Ni_7O_{5-6} are presented in Fig. S4 (ESI†). Ni_6O_4 has an unusually long lifetime compared to the other clusters (225 ± 40 fs). This extended lifetime may be related to its uniquely high C_3 symmetry (also suggested to be T_d[23]), which may facilitate the delocalization of charge carriers for a prolonged lifetime. Photoexcitation of Ni_6O_4 is unique in that it contains significant Ni-3d → O-s character (up to 0.29), which is not present in other cluster excitations. The Ni_7O_5 and Ni_7O_6 clusters have lifetimes ~29–52% greater than the expected stoichiometric lifetime of 110 fs, consistent with smaller cluster species. The transient signals for these larger clusters are presented in Fig. S5 (ESI†).

5. Conclusions

Neutral gas-phase nickel oxide clusters were produced using laser ablation and the femtosecond response to two-color pump–probe photoexcitation was measured. The sub-ps lifetimes of photoexcited states change for each cluster and depend upon the nature of the atomic orbitals involved. The stoichiometric $(NiO)_n$ clusters ($n < 6$) possess the shortest lifetimes (~110 fs) which are attributed to a LMCT and subsequent e–e scattering, similar to bulk-scale material lifetimes. Thus, electron scattering is a prominent relaxation mechanism in strongly correlated transition metal oxide clusters. This time-resolved experiment on neutral nickel oxide clusters suggests O vacancies slow relaxation by involving different atomic orbitals through photoexcitation. Decreased O content extends the sub-ps lifetime by up to 80% and allows for charge-trapping (long-lived state) through an increased Ni d → p transition character. Detailed analysis of the atomic character of the photoexcitation indicates the participation of Ni-4s orbitals are important in the ultrafast dynamics of NiO at the molecular scale. By extension, s character states cannot be ignored in the conduction band minima of bulk NiO and may be employed for extending excited state lifetimes and are therefore essential to the creation of advanced nickel oxide materials.

Author contributions

S. G. S. and J. M. G. designed the experiments. J. M. G. performed the ultrafast pump–probe spectroscopy, S. G. S. performed the theoretical calculations, and S. G. S. and J. M. G. wrote the paper.

Conflicts of interest

There are no conflicts to declare.

Acknowledgements

We gratefully acknowledge support from ASU Lightworks. J. G. also acknowledges support from Western Alliance to Expand Student Opportunities (WAESO) Louis Stokes Alliance for Minority Participation (LSAMP) Bridge to Doctorate (BD) National Science Foundation (NSF) Grant No. HRD-1702083.

References

1 M. D. Irwin, D. B. Buchholz, A. W. Hains, R. P. H. Chang and T. J. Marks, p-Type semiconducting nickel oxide as an efficiency-enhancing anode interfacial layer in polymer bulk-heterojunction solar cells, *Proc. Natl. Acad. Sci. U. S. A.*, 2008, **105**, 2783–2787.
2 A. Corani, M. H. Li, P. S. Shen, P. Chen, T. F. Guo, A. El Nahhas, K. Zheng, A. Yartsev, V. Sundström and C. S. Ponseca, Ultrafast Dynamics of Hole Injection and Recombination in Organometal Halide Perovskite Using Nickel Oxide as p-Type Contact Electrode, *J. Phys. Chem. Lett.*, 2016, **7**, 1096–1101.
3 R. J. Dillon, L. Alibabaei, T. J. Meyer and J. M. Papanikolas, Enabling Efficient Creation of Long-Lived Charge-Separation on Dye-Sensitized NiO Photocathodes, *ACS Appl. Mater. Interfaces*, 2017, **9**, 26786–26796.
4 L. Huber, A. Ferrer, T. Kubacka, T. Huber, C. Dornes, T. Sato, K. Ogawa, K. Tono, T. Katayama, Y. Inubushi, M. Yabashi, Y. Tanaka, P. Beaud, M. Fiebig, V. Scagnoli, U. Staub and S. L. Johnson, Coherent acoustic perturbation of second-harmonic generation in NiO, *Phys. Rev. B: Condens. Matter Mater. Phys.*, 2015, **92**, 94304.
5 M. Fiebig, N. P. Duong, T. Satoh, B. B. Van Aken, K. Miyano, Y. Tomioka and Y. Tokura, Ultrafast magnetization

dynamics of antiferromagnetic compounds, *J. Phys. D: Appl. Phys.*, 2008, **41**, 164005.
6 M. Fiebig, N. P. Duong, T. Satoh and T. Lottermoser, Ultrafast and magnetoelectric phase transitions in antiferromagnets, *J. Magn. Magn. Mater.*, 2006, **300**, e264–e269.
7 K. Gillmeister, D. Golež, C. T. Chiang, N. Bittner, Y. Pavlyukh, J. Berakdar, P. Werner and W. Widdra, Ultrafast coupled charge and spin dynamics in strongly correlated NiO, *Nat. Commun.*, 2020, **11**, 1–9.
8 R. Gómez-Abal, O. Ney, K. Satitkovitchai and W. Hübner, All-optical subpicosecond magnetic switching in NiO(001), *Phys. Rev. Lett.*, 2004, **92**, 227402.
9 N. Tancogne-Dejean, M. A. Sentef and A. Rubio, Ultrafast transient absorption spectroscopy of the charge-transfer insulator NiO: Beyond the dynamical Franz-Keldysh effect, *Phys. Rev. B*, 2020, **102**, 115106.
10 K. Gillmeister, M. Kiel and W. Widdra, Image potential states at transition metal oxide surfaces: A time-resolved two-photon photoemission study on ultrathin NiO films, *Phys. Rev. B*, 2018, **97**, 1–10.
11 S. Biswas, J. Husek, S. Londo and L. R. Baker, Ultrafast Electron Trapping and Defect-Mediated Recombination in NiO Probed by Femtosecond Extreme Ultraviolet Reflection-Absorption Spectroscopy, *J. Phys. Chem. Lett.*, 2018, **9**, 5047–5054.
12 E. J. Friedman-Hill and R. W. Field, Analysis of the [16.0]3Σ--X3Σ- and [16.0]3Σ--[4.3]3Πi band systems of the NiO molecule, *J. Mol. Spectrosc.*, 1992, **155**, 259–276.
13 J. L. Li, G. M. Rignanese and S. G. Louie, Quasiparticle energy bands of NiO in the GW approximation, *Phys. Rev. B: Condens. Matter Mater. Phys.*, 2005, **71**, 1–4.
14 N. Alidoust, M. C. Toroker and E. A. Carter, Revisiting photoemission and inverse photoemission spectra of nickel oxide from first principles: Implications for solar energy conversion, *J. Phys. Chem. B*, 2014, **118**, 7963–7971.
15 Y. Gao, Q. Sun, J. M. Yu, M. Motta, J. McClain, A. F. White, A. J. Minnich and G. K. L. Chan, Electronic structure of bulk manganese oxide and nickel oxide from coupled cluster theory, *Phys. Rev. B*, 2020, **101**, 1–9.
16 J. M. Garcia, R. E. Shaffer and S. G. Sayres, Ultrafast pump-probe spectroscopy of neutral Fe_nO_m clusters (n, $m < 16$), *Phys. Chem. Chem. Phys.*, 2020, **22**, 24624–24632.
17 J. M. Garcia, L. F. Heald, R. E. Shaffer and S. G. Sayres, Oscillation in Excited State Lifetimes with Size of Subnanometer Neutral $(TiO_2)_n$ Clusters Observed with Ultrafast Pump–Probe Spectroscopy, *J. Phys. Chem. Lett.*, 2021, **12**, 4098–4103.
18 J. M. Garcia and S. G. Sayres, Increased Excited State Metallicity in Neutral Cr_2On Clusters ($n < 5$) upon Sequential Oxidation, *J. Am. Chem. Soc.*, 2021, **143**, 15572–15575.
19 W. C. Wiley and I. H. McLaren, Time-of-Flight Mass Spectrometer with Improved Resolution, *Rev. Sci. Instrum.*, 1955, **26**, 1150–1157.
20 J. P. Perdew and Y. Wang, Accurate and simple analytic representation ofthe electron-gas correlation energy, *Phys. Rev. B: Condens. Matter Mater. Phys.*, 1992, **45**, 13244–13249.
21 M. Filatov and D. Cremer, Calculation of spin-densities within the context of density functional theory. the crucial role of the correlation functional, *J. Chem. Phys.*, 2005, **123**, 1–7.
22 R. H. Aguilera-Del-Toro, F. Aguilera-Granja, L. C. Balbás and A. Vega, Structure, fragmentation patterns, and magnetic properties of small nickel oxide clusters, *Phys. Chem. Chem. Phys.*, 2017, **19**, 3366–3383.
23 G. L. Gutsev, K. G. Belay, K. V. Bozhenko, L. G. Gutsev and B. R. Ramachandran, A comparative study of small 3d-metal oxide $(FeO)_n$, $(CoO)_n$, and $(NiO)_n$ clusters, *Phys. Chem. Chem. Phys.*, 2016, **18**, 27858–27867.
24 M. J. Frisch, G. W. Trucks, H. B. Schlegel, G. E. Scuseria, M. A. Robb, J. R. Cheeseman, G. Scalmani, V. Barone, B. Mennucci, G. A. Petersson, H. Nakatsuji, M. Caricato, X. Li, H. P. Hratchian, A. F. Izmaylov, J. Bloino, G. Zheng, J. L. Sonnenberg, M. Hada, M. Ehara, K. Toyota, R. Fukuda, J. Hasegawa, M. Ishida, T. Nakajima, Y. Honda, O. Kitao, H. Nakai, T. Vreven, J. A. Montgomery Jr., J. E. Peralta, F. Ogliaro, M. Bearpark, J. J. Heyd, E. Brothers, K. N. Kudin, V. N. Staroverov, R. Kobayashi, J. Normand, K. Raghavachari, A. Rendell, J. C. Burant, S. S. Iyengar, J. Tomasi, M. Cossi, N. Rega, J. M. Millam, M. Klene, J. E. Knox, J. B. Cross, V. Bakken, C. Adamo, J. Jaramillo, R. Gomperts, R. E. Stratmann, O. Yazyev, A. J. Austin, R. Cammi, C. Pomelli, J. W. Ochterski, R. L. Martin, K. Morokuma, V. G. Zakrzewski, G. A. Voth, P. Salvador, J. J. Dannenberg, S. Dapprich, A. D. Daniels, O. Farkas, J. B. Foresman, J. V. Ortiz, J. Cioslowski and D. J. Fox, *Gaussian 16, revision A.03*, Gaussian, Inc., Wallingford, CT, 2016.
25 C. J. Dibble, S. T. Akin, S. Ard, C. P. Fowler and M. A. Duncan, Photodissociation of cobalt and nickel oxide cluster cations, *J. Phys. Chem. A*, 2012, **116**, 5398–5404.
26 G. C. Nieman, E. K. Parks, S. C. Richtsmeier, K. Liu, L. G. Pobo and S. J. Riley, Multiphoton ionization and fragmentation of transition-metal cluster oxides, *High Temp. Sci.*, 1986, **22**, 115–138.
27 S. P. Walch and W. A. Goddard III, Electronic States of the NiO Molecule, *J. Am. Chem. Soc.*, 1978, **100**, 1338–1348.
28 H. Wu and L. S. Wang, A study of nickel monoxide (NiO), nickel dioxide (ONiO), and Ni(O2) complex by anion photoelectron spectroscopy, *J. Chem. Phys.*, 1997, **107**, 16–21.
29 O. Tjernberg, G. Chiaia, U. O. Karlsson and F. M. F. De Groot, Resonant photoelectron spectroscopy on CoO, *J. Phys.: Condens. Matter*, 1997, **9**, 9863–9871.
30 J. Ho, M. L. Polak, K. M. Ervin and W. C. Lineberger, Photoelectron spectroscopy of nickel group dimers: Ni-2, Pd-2, and Pt-2, *J. Chem. Phys.*, 1993, **99**, 8542–8551.
31 T. M. M. Ramond, G. E. E. Davico, F. Hellberg, F. Svedberg, P. Salén, P. Söderqvist and W. C. C. Lineberger, Photoelectron Spectroscopy of Nickel, Palladium, and Platinum Oxide Anions, *J. Mol. Spectrosc.*, 2002, **216**, 1–14.
32 V. D. Moravec and C. C. Jarrold, Study of the low-lying states of NiO- and NIO using anion photoelectron spectroscopy, *J. Chem. Phys.*, 1998, **108**, 1804–1810.

33 C. Qin, J. Zang, D. Zhang, Q. Zhang and Y. Chen,, Laser-induced Fluorescence Spectroscopy of NiO between 510 and 650 nm, *Chin. J. Chem. Phys.*, 2013, **26**, 512–518.
34 F. Ahmed and E. R. Nixon, The A → X system of Ni_2 in argon matrices, *J. Chem. Phys.*, 1979, **71**, 3547–3549.
35 M. Moskovits and J. E. Hulse, The ultraviolet–visible spectra of diatomic, triatomic, and higher nickel clusters, *J. Chem. Phys.*, 1977, **66**, 3988–3994.
36 H. Wang, H. Haouari, R. Craig, J. R. Lombardi and D. M. Lindsay, Raman spectra of mass-selected nickel dimers in argon matrices, *J. Chem. Phys.*, 1996, **104**, 3420–3422.
37 A. B. Anderson,, Theory of ultraviolet spectra for Ni_2 and Ni_3 and hypothesis for argon matrix frequency shifts for Ni atoms, *J. Chem. Phys.*, 1977, **66**, 5108–5111.
38 J. O. Noell, M. D. Newton, P. J. Hay, R. L. Martin and F. W. Bobrowicz, An ab initio study of the bonding in diatomic nickel, *J. Chem. Phys.*, 1980, **73**, 2360–2371.
39 W. Jin, C. Li, G. Lefkidis and W. Hübner, Laser control of ultrafast spin dynamics on homodinuclear iron- and nickel-oxide clusters, *Phys. Rev. B: Condens. Matter Mater. Phys.*, 2014, **89**, 1–7.
40 O. Hübner and H.-J. Himmel, MRCI investigation of Ni_2O_2 and $Ni_2O_2^+$, *Phys. Chem. Chem. Phys.*, 2009, **11**, 2241.
41 D. Vardhan, R. Liyanage and P. B. Armentrout, Guided ion beam studies of the reactions of Ni_n^+ (n = 2–18) with O_2: Nickel cluster oxide and dioxide bond energies, *J. Chem. Phys.*, 2003, **119**, 4166–4178.
42 D. Bandyopadhyay, Chemisorptions effect of oxygen on the geometries, electronic and magnetic properties of small size Ni_n (n = 1–6) clusters, *J. Mol. Model.*, 2012, **18**, 737–749.
43 L. Lian, C.-X. Su and P. B. Armentrout, Collision-induced dissociation of Ni_n^+ (n = 2–18) with Xe: Bond energies, geometrical structures, and dissociation pathways, *J. Chem. Phys.*, 1992, **96**, 7542–7554.